CHEMISTRY
A EUROPEAN JOURNAL

DOI: 10.1002/chem.200700887

On the Hydrolysis Mechanism of the Second-Generation Anticancer Drug Carboplatin

Matěj Pavelka, Maria Fatima A. Lucas, and Nino Russo*[a]

Abstract: The hydrolysis reaction mechanisms of carboplatin, a second-generation anticancer drug, have been explored by combining density functional theory (DFT) with the conductor-like dielectric continuum model (CPCM) approach. The decomposition of carboplatin in water is expected to take place through a biphasic mechanism with a ring-opening process followed by the loss of the malonato ligand. We have investigated this reaction in water and acid conditions and established that the number of protons present in the malonato ligand has a direct effect on the energetics of this system. Close observation of the optimised structures revealed a necessary systematic water molecule in the vicinity of the amino groups of carboplatin. For this reason we have also investigated this reaction with an explicit water molecule. From the computed potential-energy surfaces it is established that the water hydrolysis takes place with an activation barrier of 30 kcal mol^{-1}, confirming the very slow reaction observed experimentally. The decomposition of carboplatin upon acidification was also investigated and we have computed a 21 kcal mol^{-1} barrier to be overcome (experimental value 23 kcal mol^{-1}). We have also established that the rate-limiting process is the first hydration, and ascertained the importance of a water molecule close to the two amine groups in lowering the activation barriers for the ring-opening reaction.

Keywords: antitumor agents · cancer drug · carboplatin · cisplatin · density functional calculations · hydrolysis

Introduction

cis-Diamminedichloroplatinum(II) commonly known as "cisplatin", a square-planar platinum compound, is a well-established antitumour agent, especially effective against testicular and ovarian cancers. It has also been employed in bladder, cervical, head and neck, and small-cell lung cancer treatments.[1] However, some tumours, such as non-small-cell lung cancer, have intrinsic resistance to cisplatin, while others develop acquired resistance after the initial treatment.[2] The reasons for this resistance are not well understood, but several possible mechanisms have been identified: drug accumulation, increased repair/tolerance of platinum–DNA adducts, or alterations in proteins involved in apoptosis.[3,4] The discovery of the anticancer activity of cisplatin[5] and the need to overcome the pharmacological problems of this drug has stimulated the search for other metal-based agents such as carboplatin, oxaliplatin, trinuclear BBR 3464, or the Pt^{IV} complex JM216.[6–8] However, at present, cisplatin and carboplatin are still among the most

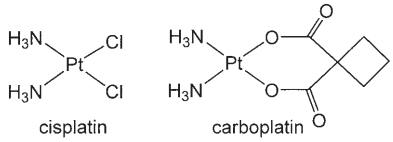

frequently used drugs.[7,9] Carboplatin presents an identical range of action to cisplatin. However, it exhibits minor neurotoxicity and nephrotoxicity. Both species are believed to exert their cytotoxicity by coordinating bifunctionally to DNA through the N(7) atoms of two adjacent guanines on the same strand (intrastrand cross-links), arresting DNA replication.[10–12] The successful development of new drugs with reduced side effects requires a correct understanding of their mechanisms of action. In the case of cisplatin, it is expected that prior to reaction with DNA it undergoes one or two hydrolysis reactions, with substitution of the chloride ions by water. This should take place when the drug passes from the blood plasma (high concentration chloride) to the cell cytoplasm (lower chloride concentration). There has

[a] Dr. M. Pavelka, M. F. A. Lucas, Prof. N. Russo
Dipartimento di Chimica Università della Calabria
Via P. Bucci, cubo 14c, 87036 Arcavacata di Rende (CS) (Italy)
Fax: (+39) 0984-492044
E-mail: nrusso@unical.it

been some discussion as to whether it is the monoaquated or the diaquated cisplatin that reacts with DNA.[13–16] Despite all the effort in understanding cisplatin reactions, to the present date it is still not known how carboplatin obstructs DNA replication. There have been some suggestions that carboplatin might function as a pre-drug of cisplatin by substitution of the cyclobutane dicarboxylate group (malonate group) by chloride groups and in this case the mode of action of carboplatin should be similar to its predecessor. However, some studies report that reaction of carboplatin with chloride ions is too slow for the reported half-life of the drug in blood plasma.[17,18]

Whether or not carboplatin is a pre-drug for cisplatin, and independently of the number of hydrolyses these drugs can undergo, the molecular structure of the DNA complex should be identical and has been solved by the Dickerson group.[19] Interstrand cisplatin cross-links are unstable under physiological conditions[20] resulting in monofunctional adducts.

As stated previously, it is expected that before creating functional complexes with DNA bases, both drugs undergo hydrolysis. In the case of cisplatin, this process is very well studied by both experimental[21–24] and theoretical tools.[25,26] The reduced toxicity of carboplatin in comparison with cisplatin is usually explained by the hydrolysis of the malonato ligand being about one order slower.[27] However, it is still not clear if the aqua species from carboplatin is in fact the active complex that reacts with DNA. Given the comparative chemical inertness of carboplatin other suggestions have been made to explain its activity. These include enzymatic activation,[28,29] reaction with sulfur nucleophiles or even direct reaction with DNA.[30] The kinetics of the ring-opening and displacement of the malonato ligand were studied within various acidic conditions.[31–34] It has been established that in acidic solution it is likely that the degradation of carboplatin should occur by a biphasic process with a first hydration leading to the ring opening, followed by a second hydration and consequent displacement of the malonate group.[33] A detailed knowledge of all stationary points involved in these reactions is important at this stage, and theoretical methods are a useful tool for obtaining a complete description of the energetics controlling this process.

The present work represents a thorough, first theoretical investigation of carboplatin hydrolysis. A number of reaction paths were studied in order to reproduce reactions in both acidic and non-acidic solutions.

Computational Methods

All calculations were performed with the Gaussian 03 quantum chemical program package.[35] Examined platinum complexes possess a singlet ground state with a total charge of 0, +1, or +2 according to the protonation states proposed by experimental tools.[31–34] All the structures were optimised using the Becke hybrid B3LYP functional.[36,37] H, C, O and N atoms we described by the 6–31G(d) basis set. For a description of the Pt atom the quasi-relativistic Stuttgart–Dresden pseudopotentials (MWB-60) were utilised.[38] The original platinum valence basis set was augmented by a set of diffuse functions: $\alpha_s=0.0075$, $\alpha_p=0.013$ and $\alpha_d=0.025$; and polarisation functions: $\alpha_f=0.98$.[39] Structure optimisations were performed at this accuracy. In order to confirm proper convergence to equilibrium and transition state geometries, vibrational frequency analyses were carried out based on analytical second derivatives of the Hamiltonian at this level of theory.

Geometry optimisations were repeated in a water environment by using the CPCM method.[40] The dominating electrostatic interaction with a continuum is provided by polarisation charges appearing on the boundary surface of the studied molecule.[41] This solvent-accessible surface was constructed using Klamt's radii[42] with explicit hydrogen atoms.

Single-point (SP) energy calculations were also carried out on the optimised structures with the larger basis set 6–31++G(2df,2pd). Platinum valence basis sets were augmented with diffuse ($\alpha_f=0.46$) and polarisation ($\alpha_g=1.21$) functions.[39,43]

Potential-energy surface (PES) profiles were estimated from total electronic energies at the 6–31++G(2df,2pd) level adding zero-point energy and enthalpy contributions at 298.15 K (ΔH^{298}). All structures presented on the PES are local minima (not global) and all reactant energies are taken as zero reference.

Net charges were computed from the natural population analyses (NPA)[44–46] method and are available in the Supporting Information.

Results

Hydrolysis in water: The first reaction studied was the decomposition of carboplatin in water. This process is expected to occur in two steps with the ring-opening of the malonato ligand followed by the release of this group. These reactions are illustrated in Scheme 1.

The potential-energy profile for reactions R1 and R2 (Scheme 1) and the optimised structures for the stationary points along R1 are displayed in Figure 1. Optimisations in solvent and in vacuo have retrieved two possible reactant structures. In the gas phase the reacting, entering water is located in proximity to the platinum centre, hydrogen bonded to one nitrogen atom from an amine group and an oxygen atom from the malonato ligand. However, in solvent this water favours the position in the vicinity of the two

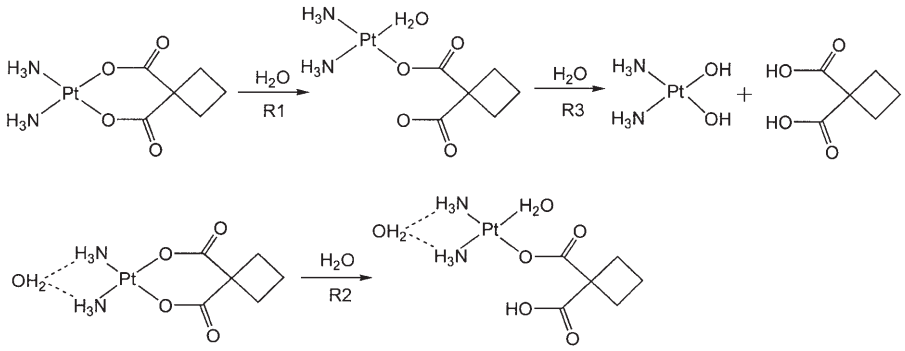

Scheme 1. Investigated paths (R1–R3) of the carboplatin ligand opening in water. The reaction depicted below (R2) refers to the system with an extra water molecule added near the amine group.

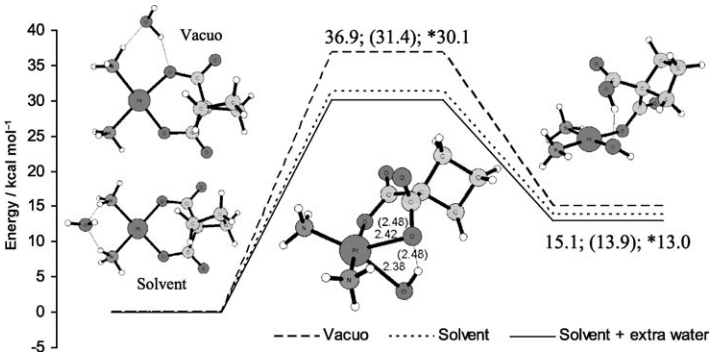

Figure 1. Energy profile and optimised structures for the addition of the first water molecule to carboplatin (R1; Scheme 1) in neutral conditions, in the gas phase, and in water. The energies for the reaction with an extra water molecule near the amine groups (R2; Scheme 1) are indicated by an asterisk. The absolute energies, in Hartree units, for the two reactant structures in the left side are −842.2933 (vacuo) and −842.2998 (water). The TS structural parameters for reaction R1 refer to the gas phase and solvent (in brackets) computations.

amine groups. Comparison of the absolute energies for these two structures at the 6–31++G(2df,2pd) level, with solvent effects included, reveals that the structure optimised in solvent is more stable than the structure optimised in vacuo by about 4 kcal mol^{-1}.

According to our calculations this reaction must overcome a 31.4 kcal mol^{-1} barrier in aqueous solution and 36.9 kcal mol^{-1} in vacuo. The transition state (TS) displays an intermediary bond length of 2.42 Å for the bond being broken between platinum (Pt) and the malonato ligand (ML) oxygen atom, and 2.38 Å for the entering water molecule. The same bonds in solvent are somewhat longer, especially for the bond being formed, (2.48 Å), but of the same magnitude. The imaginary frequency observed in the transition state, in both media, is about 230i cm^{-1}, and the animation of this vibrational mode clearly indicates the rupture of the O(ML)−Pt bond and formation of the O(water)−Pt bond. The reaction is endothermic by 14.0 and 15.1 kcal mol^{-1} in water and in the gas phase, respectively. The final product of this reaction is obtained by simultaneous scission and proton transfer from the water molecule bonded to platinum to the carboxylate group of the ligand.

Direct observation of the optimised geometries of the reactants in reactions R1 as well as R4, shown later in the results, revealed that the water molecule initially hydrogen-bonded to the amine groups has a stabilizing effect. We expect that this is more pronounced on the transition state than in the reactants, leading to a lower activation barrier. The reason for this can be understood if we take into account that the charge separation in the TS is more accentuated. For this reason, an extra water molecule added to the system acts as explicit solvent. In addition, we would suppose that a more favourable position for the reacting water molecule would be close to the Pt cation, like in R1 in vacuo. Therefore in solvent, we conducted an additional study with an extra water molecule. The optimised structures can be observed in Figure 2, which corresponds to reaction R2 in Scheme 1, and the energetic profile is displayed in Figure 1.

We can observe that the critical bond lengths in the transition-state structures are identical to the previous results for this system. The activation barrier is lowered by about 1.5 kcal mol^{-1}, retrieving a value of 30.1 kcal mol^{-1}. The endothermicity of the reaction does not change significantly, with a value of 13.0 kcal mol^{-1}.

For the next step of the reaction (R3 of Scheme 1), which leads to the loss of the malonato ligand, the addition of the second water molecule can occur in two different ways. In the first, we consider addition on the same plane as the monodentate ligand (R3A, Figure 3) or on the opposite plane, which is the second possibility (R3B, Figure 3). Optimised structures for these reactions are shown in Figure 3.

For reaction R3A, the bond lengths are more or less the same for the bond being broken and formed. We obtained an O(water)−Pt distance of 2.49 Å for the gas phase and 2.48 Å in solution for the transition state. The O(ML)−Pt distance has been estimated to be 2.49 Å in vacuo and 2.46 Å in solvent. For the addition of the water in the same plane as the ligand, in the gas phase, we calculated 2.38 Å (2.51 Å in water) for the O(ML)−Pt bond and 2.41 Å (2.50 Å in water) for the O(water)−Pt bond. The imaginary frequency for the transition state is in all cases about 200i cm^{-1}, which corresponds to the O(ML)−Pt and O(water)−Pt bonds being broken and formed, respectively. The activation barrier for the R3A reaction is 21.3 kcal mol^{-1} in water (23.5 kcal mol^{-1} for the gas phase), and that of the reaction with the addition of the water molecule in the same plane (R3B) is 22.5 kcal mol^{-1} in vacuo and 21.0 kcal mol^{-1} in solvent (see Figure 4).

The product of this reaction (Pt[$(NH_3)_2$(OH)(OH)]) is formed by the loss of the malonato ligand and concomitant proton transfer from the entering water to the leaving

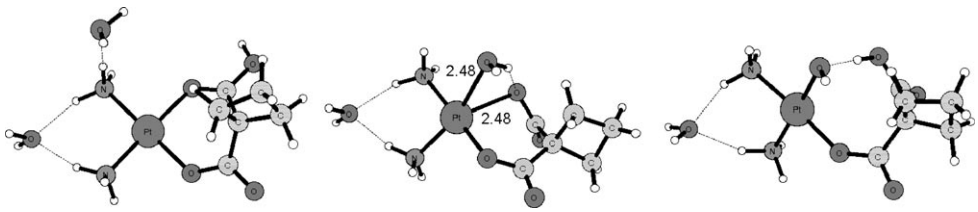

Figure 2. Optimised structures of the stationary points for the ring-opening reaction (neutral conditions) in the system with an extra water molecule near the amine groups (R2;Scheme 1). From the left: reactants, transition state and products. The indicated values are bond lengths in Angstroms.

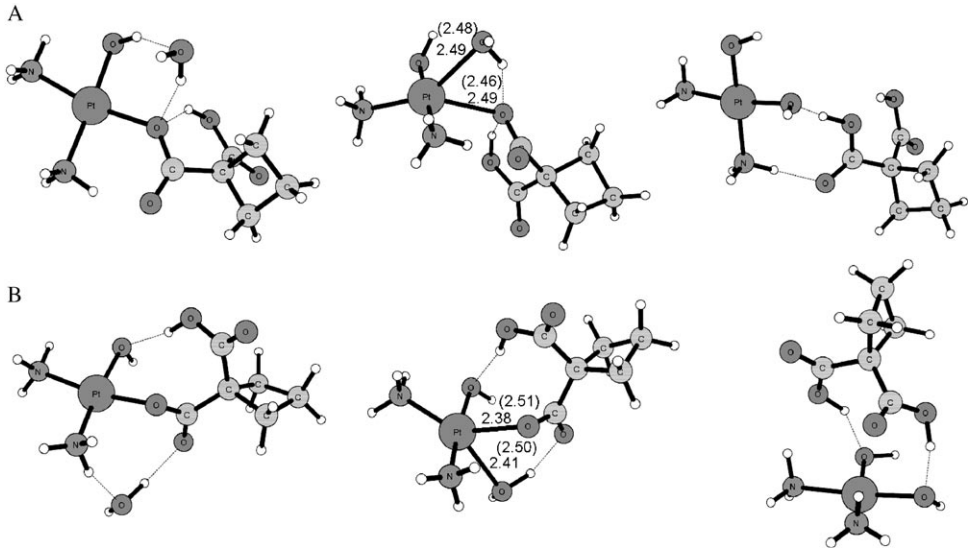

Figure 3. Optimised structures of the stationary points for the loss of the malonate group (R3, Scheme 1). A: Addition of the second water molecule in the plane opposite to the malonato ligand. B: Addition of the water molecule in the same plane as the malonato ligand.

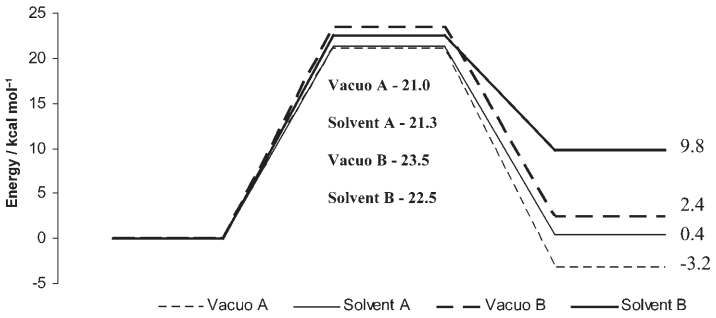

Figure 4. Energy profile for the loss of malonate group in neutral conditions (R3, Scheme 1). A and B refer to opposite or same plane of water addition, respectively.

group. From Figure 4 it emerges that reaction R3A is roughly thermoneutral (0.4 and -3.2 kcal mol^{-1} in solvent and in vacuo, respectively), while R3B is endothermic, with a greater value in solvent (9.8 kcal mol^{-1}).

These results predict that the ring-opening process should be the slowest and rate-limiting step. Kinetic experimental studies[32,33] show that the neutral hydrolysis of carboplatin is quite slow, with a reaction rate of about 5×10^{-9} s^{-1}. The ring-opening process must overcome an activation barrier of 30.1 kcal mol^{-1}, which is in excellent agreement with the experimentally expected value of about 30 kcal mol^{-1}.[33]

Hydrolysis in acidic solution: In addition to the neutral solution we also investigated carboplatin's decomposition in acid conditions. The studied paths R4 and R5 for the ring-opening process are illustrated in Scheme 2.

We initiated the calculations by adding a H_3O^+ molecule to the system, and observed that a proton is transferred with no barrier to the carboxylate group of carboplatin. Protonation is exothermic and the energy released has been estimated to be about 22 kcal mol^{-1}. The reaction must then proceed with the addition of a first water molecule and the consequent ring opening (R4 in Scheme 2). Previous experimental studies have shown that the hydrolysis of carboplatin is very slow when compared to its precursor cisplatin, but acidification of the solution increases the rate of the reaction.[27]

The optimised structures as well as the potential energy profile for the addition of a water molecule to carboplatin in acid conditions (R4) are displayed in Figure 5.

The bond length for the entering water molecule in the TS structure is 2.61 Å in the gas phase and 2.52 Å in solvent. This distance is larger than the neutral water system, especially in the gas phase. The O(ML)–Pt distance is similar to the neutral process 2.41 Å in both gas and water phases, and 2.38 and 2.48 Å for the calculations in vacuo and in neutral solvent. Observation of the imaginary frequency in the TS (about 150i cm^{-1} for both gas and solvent) confirms the expected reaction. The product of this process lies 1.8 kcal mol^{-1} above the reactants (in contrast it is slightly exothermic -2.5 kcal mol^{-1} for the gas phase) and the barriers to be surmounted are 23.4 kcal mol^{-1} for the gas phase reaction and 26.0 kcal mol^{-1} for the aqueous system. We can

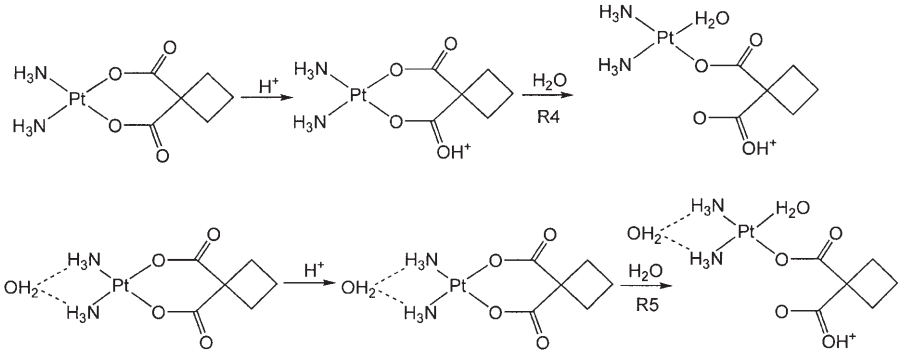

Scheme 2. Investigated paths (R4 and R5) of the carboplatin ring-opening process in acid solution. The reaction depicted below (R5) takes place with an extra water molecule hydrogen bonded to the amine groups.

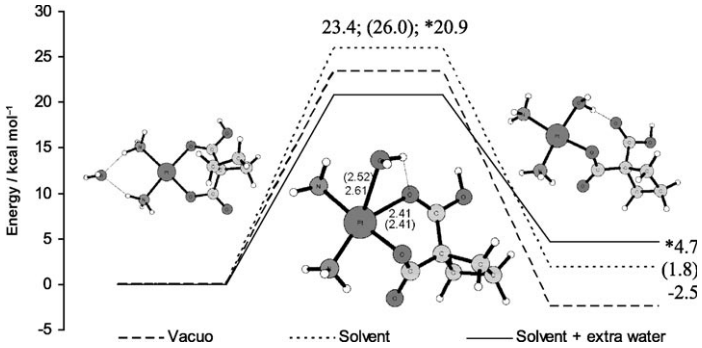

Figure 5. Energy profile and optimised structures for the addition of the first water molecule to carboplatin in acidic conditions (R4, Scheme 2), for the reactions in the gas phase and in water. The energies for the reaction with an extra water molecule near the amine groups are indicated by an asterisk. The TS structural parameters for reaction R4 are indicated for the gas phase and solvent (in brackets).

see that there is a considerable decrease in the activation energy for this step compared to the neutral system. Experimental results estimate that the highest barrier to be overcome should be about 23 kcal mol^{-1}.[33]

The reaction with an extra water molecule hydrogen bonded to the amine groups (Scheme 2, bottom) has also been studied. For reaction R2, equivalent to R1, an energy drop of 1.3 kcal mol^{-1} in the activation barrier occurred, but for R5 (equivalent to R4) the reduction was more severe, with a new activation barrier of 20.9 compared to 26.0 kcal mol^{-1} (in solvent). In spite of the energy difference, the transition state structure is quite similar to the case where this extra water molecule was not included, and the critical distances in the active site are the same (Figure 6).

The next hydration was explored following two possibilities: the direct addition of a water molecule to this system or a second protonation (strong acid conditions) on the carboxylate group prior to the displacement of the malonate group by water. These reactions are displayed in Scheme 3.

The first possibility, labelled as R6, (Scheme 3) constitutes the direct addition of a second water molecule to the platinum complex. In this case, as in R3, there are also two possibilities for the addition of the water molecule: in the same plane as the monodentate ligand, or in the opposite plane. The optimised structures as well as the energetic profile for reactions R6 are shown in Figures 7 and 8.

In R6A the water molecule adds to the complex in the opposite plane to the ligand. We note that the distance separating O(water)–Pt in vacuo, in the transition state structure, is 2.33 Å (2.44 Å in water), not so different from R4B where the distance is 2.34 Å in vacuo and 2.43 Å in solvent. The O(ML)–Pt bond is rather different with 2.46 Å for the in vacuo calculation (2.42 Å in water) compared to 2.38 Å for the addition in the same plane in the gas phase. The system determined in solution presents an identical bond length of 2.43 Å. The calculated imaginary frequency is about 200i cm^{-1} (in all reactions) and the vibrational mode corresponds to the O(ML)–Pt scission and O(water)–Pt formation. This reaction must overcome an activation barrier of 24.3 kcal mol^{-1} in water and 29.8 kcal mol^{-1} in the gas phase. For reaction R6B in water, the activation energy is 22.7 kcal mol^{-1}, slightly lower than that in vacuo, about 26.1 kcal mol^{-1}. All reactions present identical endothermicity with values ranging from 6.0 to 7.4 kcal mol^{-1}. The final product, $[Pt(NH_3)_2(OH)(H_2O)]^+$, is obtained with the loss of the malonate group.

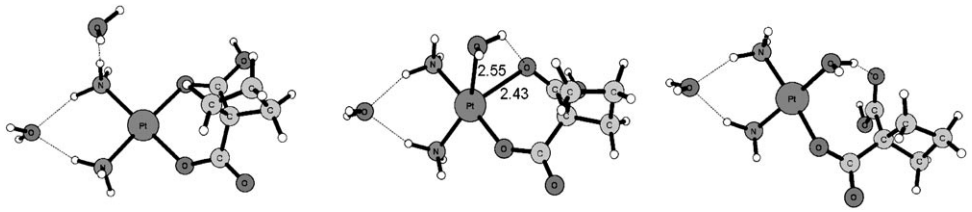

Figure 6. Optimised structures of the stationary points for the ring-opening reaction in the system with an extra water molecule near the amine groups (R5, Scheme 2) in acid conditions. From the left: reactants, transition state and products. The values included are bond lengths in Angstroms.

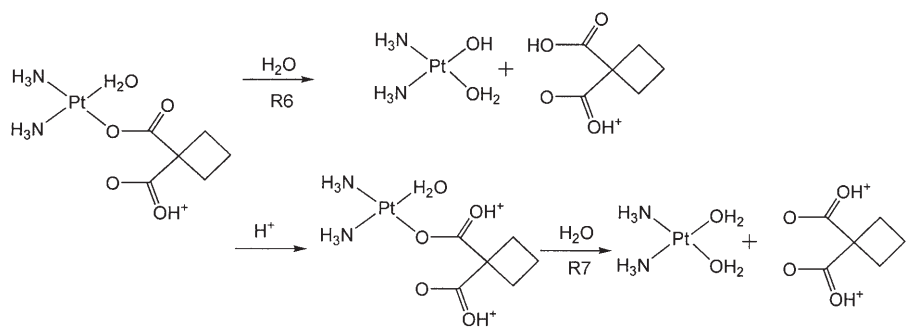

Scheme 3. Investigated paths for the loss of the malonate group in acid (R6) and strong acid conditions (R7).

We also considered the possibility of a second protonation and, in this case, we have reactions R7A and R7B, which correspond to the addition of a second water molecule (in the opposite plane and the same plane as the ligand, respectively) to the complex, but in the presence of a doubly protonated malonato ligand. The calculated energies displayed in Figure 9 are lower than the previous situation with an activation barrier of 19.2 kcal mol^{-1} for R7A, 13.5 kcal mol^{-1} for R7B in water, and 23.4 and 21.7 kcal mol^{-1}, respectively, for the gas-phase reactions.

From the potential-energy profile (Figure 9) reaction R7B in solvent is slightly exothermic

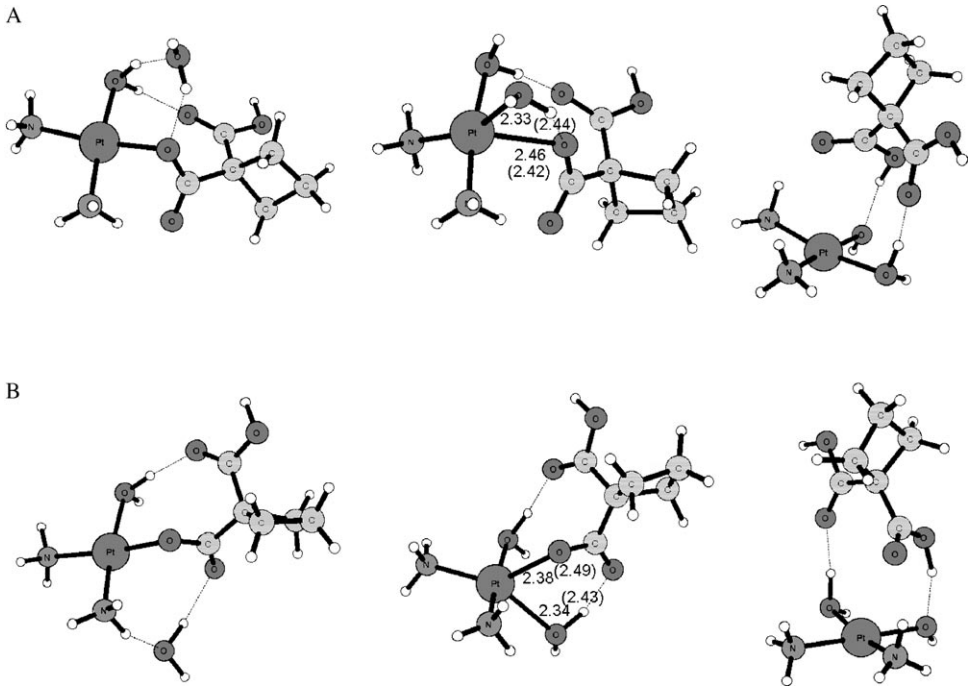

Figure 7. Optimised structures of the stationary points for the loss of the malonate group with a proton on the malonate group (R6, Scheme 3). A: Addition of the second water molecule in the plane opposite to the malonato ligand. B: Addition of the water molecule in the same plane as the malonato ligand. The structures on the left are reactants, followed by the transition states and products. All values are bond lengths in Angstroms.

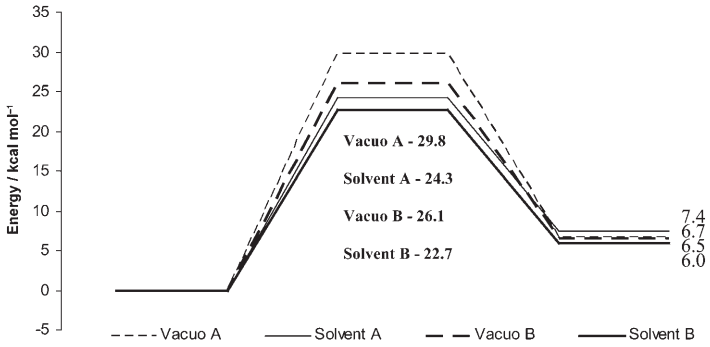

Figure 8. Energy profile for the loss of the malonate group in acidic conditions with one proton added to the system (R6, Scheme 3). A and B refer to opposite or same plane of water addition, respectively.

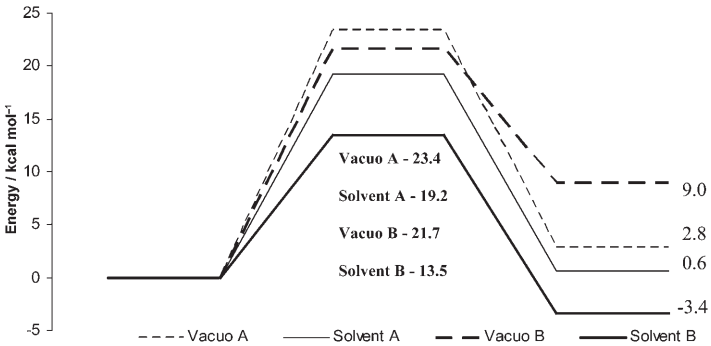

Figure 9. Energy profile for the loss of the malonate group in acidic conditions with two protons added to the system (R7, Scheme 3). A and B refer to opposite or same plane of water addition, respectively.

(−3.4 kcal mol^{-1}) and the addition of the water molecule in the same medium, but in the opposite plane is essentially thermoneutral (0.6 kcal mol^{-1}). On the other hand, both reactions in the gas phase are endothermic with a higher value for the addition of the water molecule in the same plane as the malonate group (2.8 and 9.0 kcal mol^{-1} for R7A and R7B, respectively).

From Figure 10 we can see that, for the addition in the opposite plane from the malonate group, the bond lengths between O(water)–Pt and O(ML)–Pt are essentially the same, about 2.44 Å in vacuo, but the O(water)–Pt bond length in water is slightly longer. For the addition in the same plane the O(water)–Pt distance is longer than the O(ML)–Pt distance in both solvent and gas phases.

The vibrational mode associated with the imaginary frequency (for all reactions in the order of 150i cm^{-1}) clearly indicates that the O(water)–Pt bond is being formed and the O(ML)–Pt bond broken.

From these results, the lowest energy profile proceeds by R4 and R7B, and the product of this reaction upon malonate group loss is a double aqua complex Pt[$(NH_3)_2$-$(H_2O)_2$]$^{2+}$.

Discussion

Experimental studies propose a biphasic reaction, involving a ring-opening of the malonato ligand followed by the loss of the monodentate ligand. According to the results here obtained, reaction should be initiated by a protonation of the malonate group. This protonation is accompanied by a 22 kcal mol^{-1} energy loss. We have observed that it is important that the amine groups are adequately stabilised by a water molecule. The ring-opening process is promoted by the addition of the first water molecule. From the energetics we expect a second protonation on the malonate group to take place prior to the addition of the second water molecule. The malonate group is then released and the product is formed. We have investigated all reaction paths, in both gas and water phases, and observed significant differences between the optimised structures as well as the energetics. It is interesting to observe that the solvent usually has the effect of lowering the activation barriers. In Figure 11, the solvent influence on carboplatin's structure is illustrated. The more

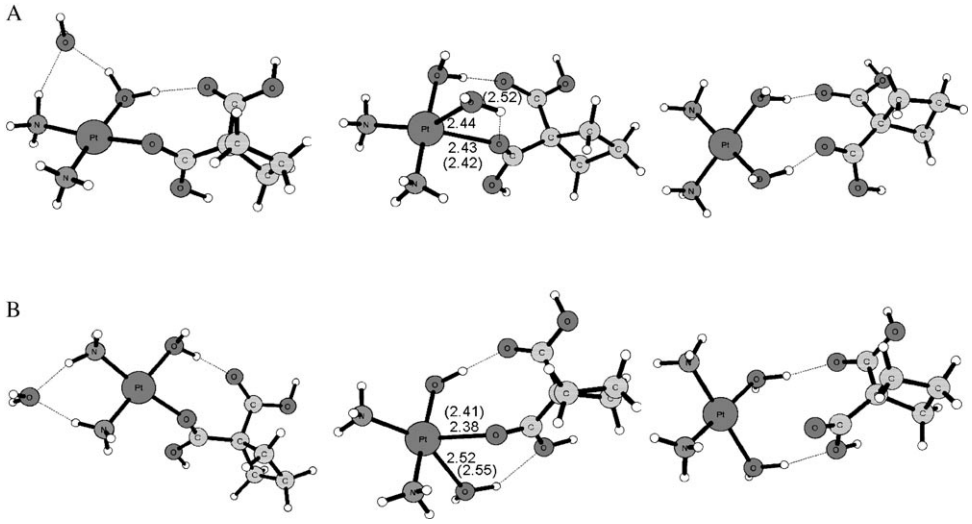

Figure 10. Optimised structures of the stationary points for the loss of the malonate group with two protons on the malonate group (R7, Scheme 3). A: Addition of the second water molecule in the plane opposite to the malonato ligand. B: Addition of the water molecule in the same plane as the malonato ligand. The structures on the left are reactants, followed by the transition states and products. All values are bond lengths in Angstroms.

cess and must overcome a 21 kcal mol^{-1} activation barrier, which is in excellent agreement with the experimental activation barrier of about 23 kcal mol^{-1} for the hydrolysis of carboplatin in acidic conditions. The loss of the malonate group takes place with a 13 kcal mol^{-1} activation barrier in the presence of two protons on the carboxylate groups. We have established that the decomposition of carboplatin in neutral water solution is much slower than in acid conditions and a 30 kcal mol^{-1} activation barrier has been computed (the same value is expected experimentally).

Solvent effects can be also recognised from the platinum

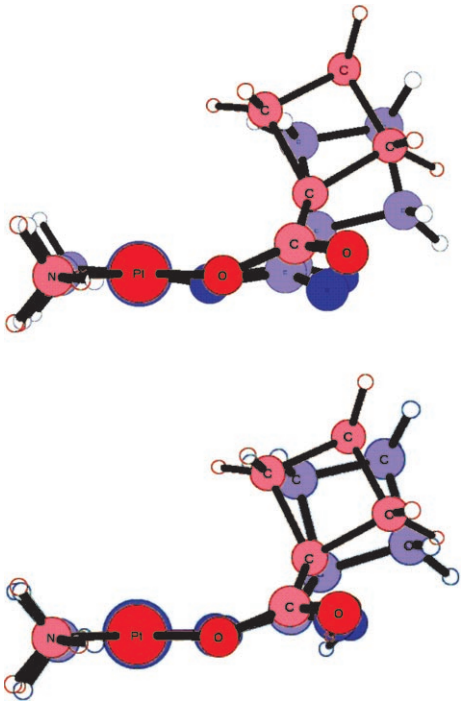

Figure 11. Illustrations of solvent influence on carboplatin structure (for non-protonated and protonated state). Blue and red colours represent structures optimised in vacuo and in water, respectively.

Table 1. Coordination distances [Å] for non-protonated (X) and protonated (X·H$^+$) carboplatin.

	In vacuo		In water	
	X	X·H$^+$	X	X·H$^+$
Pt–N_1	2.099	2.103	2.065	2.062
Pt–N_2	2.098	2.058	2.065	2.038
Pt–O_1	1.987	2.045	2.025	2.059
Pt–O_2	1.986	1.983	2.023	2.025

coordination distances presented in Table 1. We can see that the Pt–O(monodentate) bonds elongate after solvation. Such a bond has strong electrostatic character, which is screened in the presence of a water continuum. The weaker malonato ligand coordination results in shorter Pt–N(amine) distances in solvent structures. In the case of protonated carboplatin (X·H$^+$), there is also evidence for the *trans* effect: the protonated carboxylate group makes a weaker and longer Pt–O bond, resulting in a shorter bond with the opposite NH_3 ligand. The *trans* effect is also well documented for the cisplatin drug.[43]

Conclusion

In the present work, we have performed a mechanistic study of the hydration processes of carboplatin, a second-generation anticancer drug of cisplatin.

We initiated the study by investigating the reaction profile of the degradation in water, which is known to be very slow. The calculated activation barrier is 30.1 kcal mol^{-1}, which is in excellent agreement with the experimental value of

"bowed" malonato ligand in the water environment leads to easier formation of hydrogen bonds in proximity to the Pt cation.

The lowest energy profile was obtained in acid conditions. The ring-opening reaction should be the rate-limiting pro-

30 kcal mol^{-1}. The decomposition occurs in two steps, with the ring opening as the slowest and rate-limiting process, followed by the loss of the ligand, which takes place significantly faster. We followed the addition of the second water molecule in two possible positions: in the same plane as the ligand, and in the opposite plane. We were able to establish that addition in the opposite plane to the ligand occurs with a lower activation barrier. The product of this reaction is Pt-[$(NH_3)_2$(OH)(OH)], formed with the loss of the malonate group and concomitant proton transfer from the second entering water to the exiting ligand.

Upon acidification, the activation barriers are lowered. The addition of a H_3O^+ molecule induced a spontaneous proton transfer to a negatively charged oxygen atom on the malonate group. We have established that in acidic conditions the rate-limiting process is still the first water addition, with a calculated activation energy of 26 kcal mol^{-1} (experimental value 23 kcal mol^{-1}). We have also established that this barrier is considerably lowered if a water molecule is added to the system in close proximity to the amino groups. The presence of this extra water leads to an activation process of only 21 kcal mol^{-1}. Once the ring-opening process is complete the addition of the second water molecule should take place in the same plane as the ligand with an activation energy of 13.5 kcal mol^{-1}, in strong acid conditions.

This study has allowed a better understanding of the mechanisms controlling carboplatin hydrolysis, and we were able to observe considerable differences relative to its predecessor cisplatin. Cisplatin can undergo two hydrolyses, but the second hydration takes place with a higher activation barrier and for this reason many studies have suggested that cisplatin should bind to DNA monohydrated. However, calculations on carboplatin have shown that the first hydration is much slower than the second, and for this reason we expect that the second hydration should take place prior to reaction with DNA. In addition, the presence of the malonate group can lead to large stereochemical impediments that do not occur in the case of cisplatin. From these results, if carboplatin undergoes a hydration process prior to reaction with DNA, then it should be doubly hydrated.

Acknowledgement

Financial support from the Università della Calabria and Regione Calabria (POR Calabria 2000/2006 misura 3.16 progetto PROSICA) is gratefully acknowledged.

[1] G. Giaccone, *Drugs* **2000**, *59*, 9.
[2] R. P. Perez, *Eur. J. Cancer* **1998**, *34*, 1535.
[3] G. Chu, *J. Biol. Chem.* **1994**, *269*, 787.
[4] L. R. Kelland, *Drugs* **2000**, *59*, 1.
[5] B. Rosenberg, L. Van Camp, T. Krigas, *Nature* **1965**, *205*, 698.
[6] H. Zorbas, B. K. Keppler, *ChemBioChem* **2005**, *6*, 1157.
[7] D. Wang, S. J. Lippard, *Nat. Rev. Drug Discovery* **2005**, *4*, 307.
[8] M. A. G. Jakupec, B. K. Keppler, *Rev. Physiol. Biochem. Pharmacol.* **2003**, *146*, 1.
[9] W. Kaim, B. Schwederski, *Bioinorganic Chemistry: Inorganic Elements in the Chemistry of Life*, Wiley, Chichester (UK), **1994**.
[10] J. Reedijk, *Pure Appl. Chem.* **1987**, *59*, 181.
[11] S. E. Sherman, S. J. Lippard, *Chem. Rev.* **1987**, *87*, 1153–1181.
[12] M. A. A. Fuertes, J. M. Pérez, *Chem. Rev.* **2003**, *103*, 645.
[13] M. S. Davies, S. J. Berners-Price, T. W. Hambley, *Inorg. Chem.* **2000**, *39*, 5603.
[14] J. Raber, C. Zhu, L. A. Eriksson, *Mol. Phys.* **2004**, *102*, 2537.
[15] M. W. G. De Bolster, R. Cammack, D. N. Coucouvanis, J. Reedijk, C. J. Veeger, *J. Biol. Inorg. Chem.* **1996**, *1*, G1.
[16] F. Legendre, V. Bas, J. Kozelka, J.-C. Chottard, *Chem. Eur. J.* **2000**, *6*, 2002.
[17] M. A. Allsopp, G. J. Sewell, C. G. Rowland, C. M. Riley, R. L. Schowen, *Int. J. Pharm.* **1991**, *69*, 197.
[18] L. Canovese, L. Cattalini, G. Chessa, M. L. Tobe, *J. Chem. Soc. Dalton Trans.* **1988**, 2135.
[19] R. M. Wing, P. Pjura, H. R. Drew, R. E. Dickerson, *EMBO J.* **1984**, *3*, 1201.
[20] C. Perez, M. Leng, J. M. Malinge, *Nucleic Acids Res.* **1997**, *25*, 896.
[21] J. Arpalahti, M. Mikola, S. Mauristo, *Inorg. Chem.* **1993**, *32*, 3327.
[22] K. Hindmarsh, D. A. House, M. M. Turnbull, *Inorg. Chim. Acta* **1997**, *257*, 11.
[23] M. Mikola, J. Arpalahti, *Inorg. Chem.* **1994**, *33*, 4439.
[24] J.-L. Jestin, B. Lambert, J.-C. Chottard, *J. Biol. Inorg. Chem.* **1998**, *3*, 515.
[25] D. V. Deubel, *J. Am. Chem. Soc.* **2006**, *128*, 1654.
[26] J. V. Burda, M. Zeizinger, J. Leszczynski, *J. Comput. Chem.* **2005**, *26*, 907.
[27] J. J. Roberts, R. Knox, F. Friedlos, D. A. Lydall, *Biochemical Mechanisms of Platinum Antitumour Drugs* (Eds: D. C. H. McBrien, T. F. Slater), IRL, Oxford, **1986**, p. 29.
[28] M. J. Cleare, P. C. Hydes, B. W. Malerbi, D. M. Watkins, *Biochimie* **1978**, *60*, 835.
[29] M. J. Cleare, *Coord. Chem. Rev.* **1974**, *12*, 349.
[30] R. J. Knox, F. Friedlos, D. A. Lydall, J. J. Roberts, *Cancer Res.* **1986**, *46*, 1972.
[31] L. Canovese, L. Cattalini, G. Chesa, M. L. Tobe, *J. Chem. Soc. Dalton Trans.* **1988**, 2135.
[32] U. Frey, J. D. Ranford, P. J. Sadler, *Inorg. Chem.* **1993**, *32*, 801.
[33] R. W. Hay, S. Miller, *Polyhedron* **1998**, *17*, 2337.
[34] E. Curis, *New J. Chem.* **2000**, *24*, 1003.
[35] Gaussian 03 (Revision C.2), M. J. Frisch, G. W. Trucks, H. B. Schlegel, G. E. Scuseria, M. A. Robb, J. R. Cheeseman, J. A. Montgomery Jr., T. Vreven, K. N. Kudin, J. C. Burant, J. M. Millam, S. S. Iyengar, J. Tomasi, V. Barone, B. Mennucci, M. Cossi, G. Scalmani, N. Rega, G. A. Petersson, H. Nakatsuji, M. Hada, M. Ehara, K. Toyota, R. Fukuda, J. Hasegawa, M. Ishida, T. Nakajima, Y. Honda, O. Kitao, H. Nakai, M. Klene, X. Li, J. E. Knox, H. P. Hratchian, J. B. Cross, C. Adamo, J. Jaramillo, R. Gomperts, R. E. Stratmann, O. Yazyev, A. J. Austin, R. Cammi, C. Pomelli, J. W. Ochterski, P. Y. Ayala, K. Morokuma, G. A. Voth, P. Salvador, J. J. Dannenberg, V. G. Zakrzewski, S. Dapprich, A. D. Daniels, M. C. Strain, O. Farkas, D. K. Malick, A. D. Rabuck, K. Raghavachari, J. B. Foresman, J. V. Ortiz, Q. Cui, A. G. Baboul, S. Clifford, J. Cioslowski, B. B. Stefanov, G. Liu, A. Liashenko, P. Piskorz, I. Komaromi, R. L. Martin, D. J. Fox, T. Keith, M. A. Al-Laham, C. Y. Peng, A. Nanayakkara, M. Challacombe, P. M. W. Gill, B. Johnson, W. Chen, M. W. Wong, C. Gonzalez, J. A. Pople, Gaussian, Inc., Pittsburgh, PA, **2004**.
[36] A. D. Becke, *J. Chem. Phys.* **1993**, *98*, 5648.
[37] C. T. Lee, W. T. Yang, R. G. Parr, *Phys. Rev. B* **1988**, *37*, 785.
[38] D. Andrae, U. Haussermann, M. Dolg, H. Stoll, H. Preuss, *Theor. Chim. Acta* **1990**, *77*, 123.
[39] J. V. Burda, M. Zeizinger, J. Sponer, J. Leszczynski, *J. Chem. Phys.* **2000**, *113*, 2224–2232.
[40] A. Klamt, F. Eckert, M. Hornig, M. E. Beck, T. Burger, *J. Comput. Chem.* **2002**, *23*, 275.
[41] J. Tomasi, R. Cammi, B. Mennucci, C. Cappelli, S. Corni, *Phys. Chem. Chem. Phys.* **2002**, *4*, 5697.

[42] A. Klamt, V. Jonas, T. Burger, J. C. W. Lohrenz, *J. Phys. Chem. A* **1998**, *102*, 5074.
[43] M. Pavelka, J. V. Burda, *J. Mol. Model.* **2007**, *13*, 367.
[44] J. P. Foster, F. Weinhold, *J. Am. Chem. Soc.* **1980**, *102*, 7211.
[45] A. E. Reed, F. Weinhold, *J. Chem. Phys.* **1983**, *78*, 4066.
[46] A. E. Reed, R. B. Weinstock, F. Weinhold, *J. Chem. Phys.* **1985**, *83*, 735.

Received: June 12, 2007
Published online: September 25, 2007

